J Supercond Nov Magn (2012) 25:1501–1507
DOI 10.1007/s10948-012-1412-9

ORIGINAL PAPER

Fabrication and Properties of Ag–Ni Bimetallic Sheathed (Bi,Pb)-2223 Tapes

X.P. Chen · X.W. Yu · M. Liu · M.Y. Li · H.B. Sun · Q. Liu

Received: 19 December 2011 / Accepted: 3 January 2012 / Published online: 19 January 2012

Abstract 10-meter-long Ag–Ni bimetallic sheathed (Bi,Pb)-2223 tapes with outer nickel sheath and inner silver sheath have been successfully fabricated by the "Powder in tube" technique. Microstructure and phase evolution studies by means of SEM and XRD, as well as critical current density (J_c) measurements have been performed. It is found that the nickel sheath and dwell time in the first sintering process have great influences on the texture evolution, phase transformation and J_c of the Bi-2223/Ag/Ni tapes. Mono-filament (Bi,Pb)-2223 tape with a J_c of 6656 A cm^{-2} and 61-filament tape with a J_c of 12420 A cm^{-2} are obtained. Although using composite bimetallic sheaths can reduce production costs and improve mechanical properties of the Bi-2223 tapes, the Bi-2223 content and J_c of Bi-2223/Ag/Ni tapes are relatively lower than that of traditional Bi-2223/Ag tapes. Meanwhile, due to higher Bi-2223 content and better alignment of Bi-2223 grains, tapes with 61-filament have higher J_c than mono-filament tapes.

Keywords (Bi,Pb)-2223/Ag/Ni tapes · Bimetallic sheathes · Critical current density · Dwelling time

X.P. Chen (✉) · X.W. Yu · M. Liu · Q. Liu
College of Materials Science and Engineering, Chongqing University, Chongqing 400030, China
e-mail: xpchen@cqu.edu.cn

M.Y. Li
Department of Materials Science and Engineering, Northeastern University at Qinhuangdao, Qinhuangdao 066004, China

H.B. Sun
Innova Superconductor Technology Co., Ltd, Beijing 100176, China

1 Introduction

Silver-sheathed (Bi,Pb)-2223 ((Bi,Pb)-2223/Ag) superconducting tapes have been used in various devices, such as cables, magnets, transformers and current limiters because of their high current carrying capability and simple fabrication process for manufacturing long-length tapes [1–7]. In the fabrication of the tapes, silver and silver alloys, which act as stabilizers and supports, are sintered at high temperature for more than 100 hours, therefore, the (Bi,Pb)-2223/Ag tapes usually have poor mechanical properties [8, 9]. When the tapes are used, especially in a magnetic field, a large electromagnetic force will be generated and applied to the tapes due to their high critical current density (J_c) [10]. Because of the poor mechanical properties, conventional (Bi,Pb)-2223/Ag tapes may not be used in a high magnetic field. Though significant reinforcement could be achieved by soldering hard metal strips, such as brass and steel, onto one or two sides of the tapes [11, 12], the reinforced tapes cannot be heat-treated again because of the low melting points of the solders. In addition, the production costs of the (Bi,Pb)-2223/Ag tapes are too high for large-scale applications [13, 14]. However, drastic cost reduction can be realized by using other metals instead of silver alloys, which are a predominant contributor to the production costs of the (Bi,Pb)-2223/Ag tapes. Using alternative types of high strength metal instead of silver alloy as the outer sheath will also increase the mechanical properties of the (Bi,Pb)-2223/Ag tapes.

Unfortunately, most metals tend to be oxidized and some metals can contaminate the ceramic cores by diffusing through the silver sheath during long-term heat-treating processes. However, it is reported that in composite Ag–Ni ribbons, which are used as substrates for Bi-2212 tapes, Ag can prevent the diffusion of Ni toward the Bi-2212 layer [15, 16]. Thereafter, Ag–Ni composite-sheathed Bi-2223

tapes using Ni as the outer sheath were successfully manufactured by Grivel et al. [17] and Li et al. [18]. Though this tape is promising for enhancing mechanical properties and reducing production costs, tapes with long length and multi-filament core have not yet been successfully fabricated. Due to the importance of heat-treatment conditions [19–21], more studies, such as ones demonstrating suitable microstructure and texture evolution of the tapes, ought to be performed to optimize the heat-treatment conditions and improve the properties of Ag–Ni bimetallic sheathed (Bi,Pb)-2223 tapes.

In this paper, mono- and 61-filament Ag–Ni bimetallic sheathed (Bi,Pb)-2223 tapes were successfully fabricated. At the same time, the influence of some conditions, including the outer Ni sheath and annealing time in the first sintering process, on the J_c and the evolution of microstructure and texture were studied. Also, the differences between the mono- and 61-filament tapes were analyzed. Finally, a detailed discussion on the microstructure and texture evolution of the mono- and 61-filament tapes was performed based on SEM and XRD results.

2 Experimental details

Ag–Ni bimetallic sheathed (Bi,Pb)-2223 green tapes were successfully fabricated by the Powder-In-Tube technique. A silver tube (OD 8 mm, ID 6 mm) which was filled with precursor powder was drawn to a wire with outer diameter of 2.98 mm. The nominal composition of the precursor powder was $Bi_{1.8}Pb_{0.33}Sr_{1.87}Ca_{2.0}Cu_{3.0}O_{10+\delta}$. This attained wire was placed inside a Ni tube (OD 4 mm, ID 3.2 mm) and the composite wire was deformed into a tape with a thickness of 0.5 mm. A 61-filament wire (OD 3 mm) was placed inside a Ni tube (OD 4 mm, ID 3.2 mm). This composite wire was deformed into a tape with a thickness of 0.5 mm as well. Overall shape of the mono- and 61-filament Ag–Ni bimetallic sheathed (Bi,Pb)-2223 green tapes over 10 m could be seen in Fig. 1. Samples with different filaments were cut down from the long tapes and the size was 0.5 mm thick, 4.2 mm wide, ∼40 mm long.

For realizing the Ag sheath can directly contact with outer atmosphere, one edge of the samples was removed. The samples underwent the first sintering process that sintered at 837°C for 30, 40 and 50 h in an atmosphere of 8.5% O_2 (rest N_2) with heating and cooling rate of 100°C/h. After the first sintering, all samples were pressed and underwent the second sintering. The second sintering was processed at 837°C and lasted for 30 h. Subsequently, the sintering temperature was lowered to 790°C at a rate of 0.5°C/h and then reduced to room temperature at a rate of 100°C/h.

(Bi,Pb)-2223 fraction after the first and second sintering were detected by X-ray diffraction (XRD) which was carried out using Cu Kα radiation on the flat surface of the ceramic core after peeling away the metal sheaths. The degree of the texturing was evaluated by the full width at half maxi-mum (FWHM) along the rolling direction of the (0 0 14) pole intensity normal to the rolling plane [22]. Transversal cross-section images of tapes were observed on a Nova 400 Nano-SEM in the backscattered electron (BSE) imaging mode. Critical current (I_c) of samples were measured by standard four-point technique with a criterion of 1 $\mu V\,cm^{-1}$.

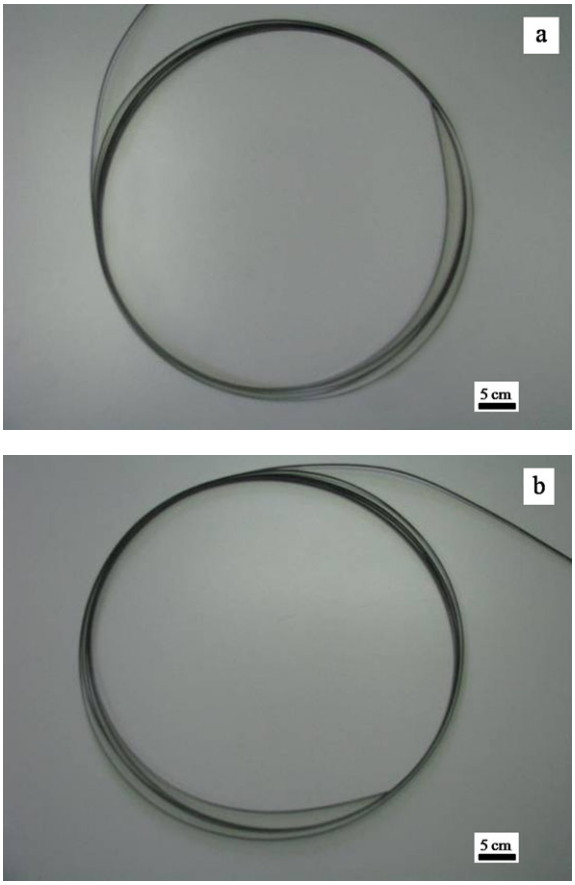

Fig. 1 The overall shapes of long (**a**) mono-filament and (**b**) 61-filament Ag–Ni bimetallic sheathed (Bi,Pb)-2223 green tape

3 Results and discussion

Figure 1 shows overall shapes of the 10 m long mono- and 61-filament green tapes fabricated by the PIT method. It is presented in Fig. 1 that the Ag–Ni bimetallic sheathed (Bi,Pb)-2223 tapes can be manufactured long enough for commercial use. Transversal and longitudinal cross-section images of the mono- and 61-filament (Bi,Pb)-2223 Ag–Ni green tapes are shown in Fig. 2(a–d). The transversal cross-section images of the mono- and 61-filament tapes are demonstrated in Fig. 2(a) and (b). The white and black regions are the Ag layer and the ceramic core, respectively,

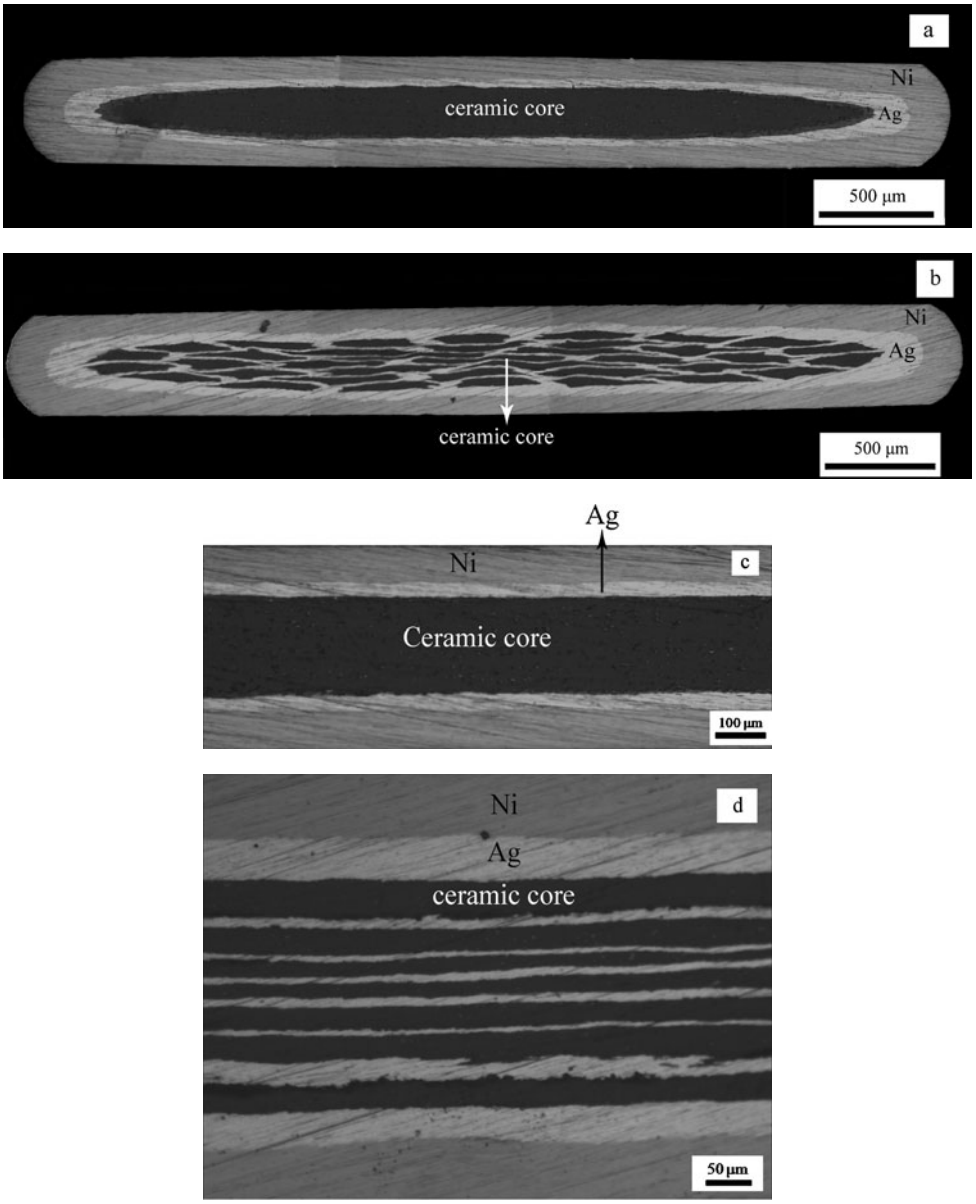

Fig. 2 Transversal and longitudinal cross-section images of mono- and 61-filament Ag–Ni bimetallic sheathed (Bi,Pb)-2223 green tapes. (**a**) Transversal cross-section image of mono-tape. (**b**) Transversal cross-section image of 61-filament tape. (**c**) Longitudinal cross-section image of mono-tape. (**d**) Longitudinal cross-section image of 61-filament tape

and the outer sheath is Ni. The thickness of the Ag sheath in the mono-filament tape and 61-filament tape are 32.3 and 37.3 μm, respectively. However, due to the finite diffusing depth of Ni toward Ag during sintering periods [15, 17], the thickness of Ag layer can be much thinner in industrial production. Meanwhile, Figs. 2(c) and (d) present the longitudinal cross-section photographs of the two style tapes showing inconspicuous "sausaging effect" caused by rolling. However, due to a higher density of the ceramic cores [23], the "sausaging effect" in the 61-filament tape is much more apparent compared to the mono-filament tape.

J_c and (Bi,Pb)-2223 fraction of the mono- and 61-filament tapes after the first sintering process are illustrated in Figs. 3 and 4. It is clearly seen that the J_c of the mono- and 61-filament tapes which are near to zero after sintered for 30 h present the same tendency that increasing with the sintering time extension, this phenomenon largely results from the increase of the (Bi,Pb)-2223 fraction (Fig. 4). Nevertheless, because much more direct contacts between Ag and ceramic cores accelerate the formation of the (Bi,Pb)-2223 and the regions near the Ag sheath have a faster phase transforming rate [24, 25], the 61-filament tapes therefore

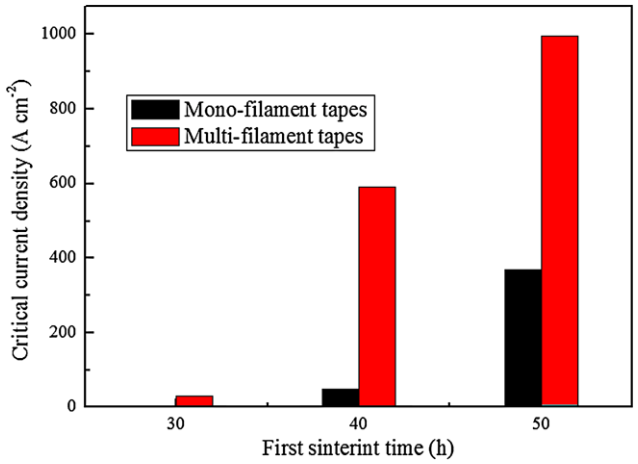

Fig. 3 The critical current density of the mono- and 61-filament tapes with the different annealing time in the first sintering

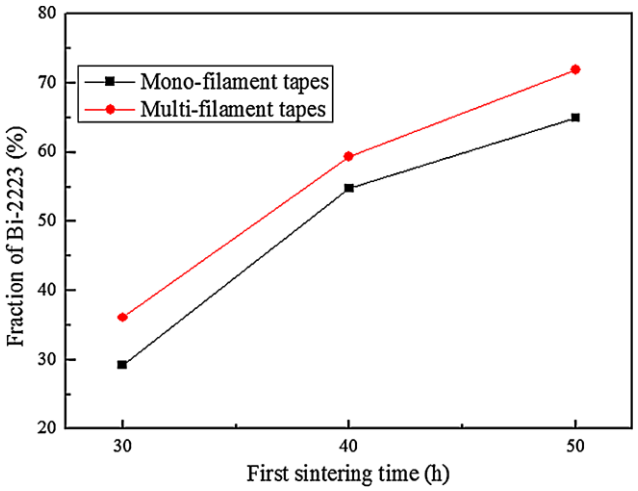

Fig. 4 The (Bi,Pb)-2223 contents of the mono- and 61-filament tapes after first sintering process

have higher (Bi,Pb)-2223 contents and J_c. After sintered for 50 h, the J_c of the mono- and 61-filament tapes reach to 368 and 995 A cm^{-2}, respectively. However, both the fraction of (Bi,Pb)-2223 in the (Bi,Pb)-2223/Ag/Ni tapes and the J_c of that are much lower than those in the (Bi,Pb)-2223/Ag tapes. Chen et al. [26] reported that the (Bi,Pb)-2223 fraction in the mono-filament (Bi,Pb)-2223/Ag tape can reach to 90% and the J_c of that achieved to 2784 A cm^{-2} after sintered for 20 h. The differences between the Ag–Ni sheathed and Ag sheathed (Bi,Pb)-2223 tapes will be mainly ascribed to the low diffusion of O_2 restrained by the outer Ni sheath, even if one edge of the Ni sheath is grinded off.

Besides the content, the alignment of the (Bi,Pb)-2223 grains also has an important influence on the J_c [24, 27]. Figure 5 presents the texture evolution of the (Bi,Pb)-2223 grains in the mono- and 61-filament tapes with different sintering time recorded by rocking curves. It is evident that

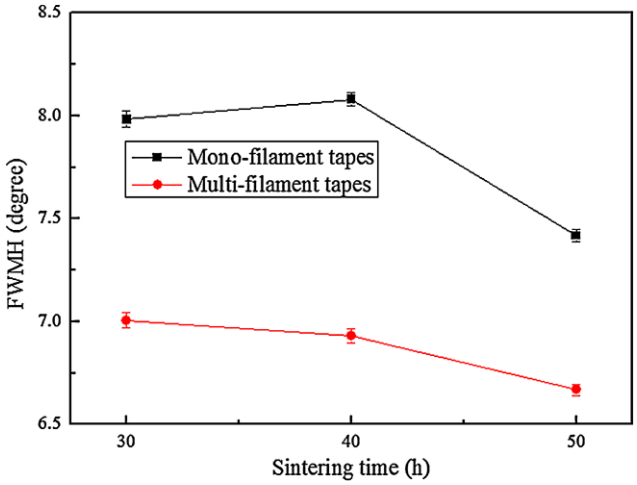

Fig. 5 The FWHM evolution of (Bi,Pb)-2223 grains in mono- and 61-filament tapes recorded by rocking curves with different dwell time in the first sintering

FWHM values of the 61-filament tapes are lower than that of the mono-filament tapes with the same sintering time, which means that the (Bi,Pb)-2223 grains in the 61-filament tapes align better. This is mainly attributed to the orientation of new (Bi,Pb)-2223 grains follows that of the original Bi-2212 grains which are aligned better in the 61-filament green tapes [28–30]. Meanwhile, the FWHM values of the mono- and 61-filament tapes decrease with the sintering time extension, which can be ascribed to the growth of the (Bi,Pb)-2223 grains within the a–b plane.

Figure 6 shows the transversal cross-section microstructures of the mono-filament tape after the first sintering process with the dwelling time of 40 h. The outer and middle layers are the Ni and Ag sheaths, respectively, and the areas surrounded by Ag are the ceramic core (see Fig. 6(a)). Figure 6(b) and (c) show the microstructures of the ceramic cores at different areas. The white regions are regarded as the lead-rich phases, the dark grey and light grey areas are the (Bi,Pb)-2223 and (Bi,Pb)-2212 phases, respectively, while the black particles are alkaline-earth cuprate or CuO grains. It is clearly seen that the regions close to and away from the Ni opening are occupied by the (Bi,Pb)-2223 grains, as is also shown in the XRD results.

Microstructures of the 61-filament tapes after the first sintering process with different dwelling time are observed in Fig. 7. The (Bi,Pb)-2223 grains, which are very few within 30 h sintering (Fig. 7(a)), increase with the extension of sintering time (seen in Figs. 7(b) and (c)). Meanwhile, the sample sintered for 40 h produce few and small secondary phases while some large secondary phase particles appear in the samples sintered for 30 and 50 h.

The J_c of the fully reacted tapes are shown in Fig. 8. Obviously, the mono-filament tape dwelled for 30 h in the first sintering process has the maximum J_c, with a value

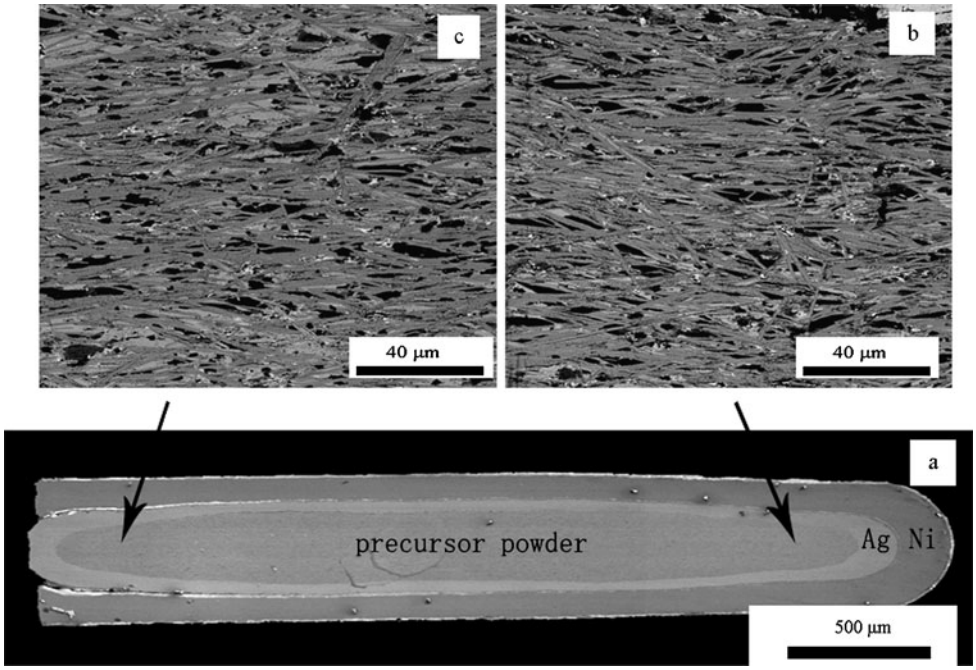

Fig. 6 Transversal cross-section images of mono-filament Ag–Ni bimetallic sheathed (Bi,Pb)-2223 tapes after sintered for 40 h: (**a**) overall shape, (**b**) far from the opening, (**c**) near the opening

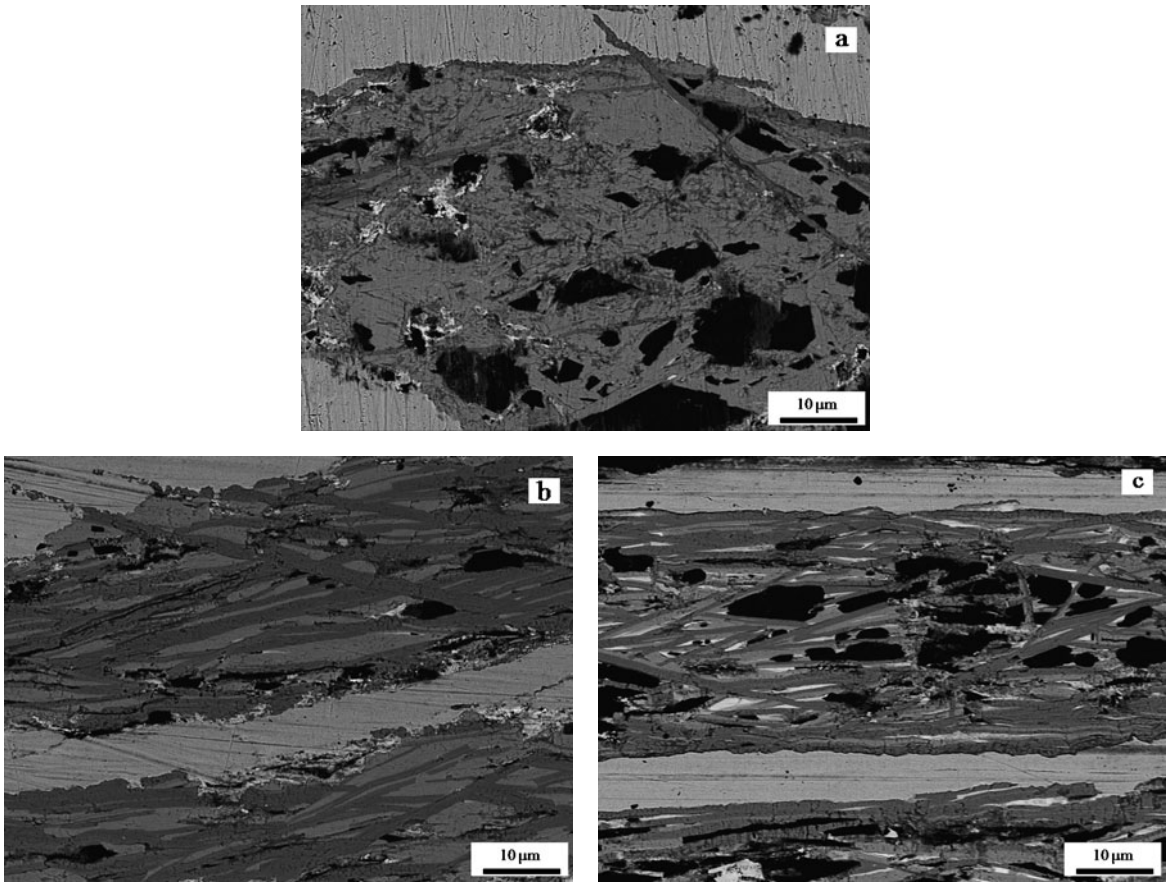

Fig. 7 Transversal cross-section images of 61-filament Ag–Ni bimetallic sheathed (Bi,Pb)-2223 tapes after first sinter for different time: (**a**) 30 h, (**b**) 40 h, (**c**) 50 h

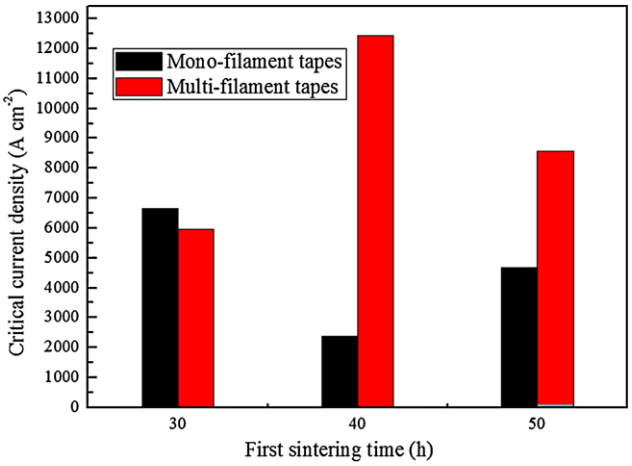

Fig. 8 The critical current density of fully reacted mono- and 61-filament tapes with different annealing time in the first sintering

of 6656 A cm^{-2}. However, the 61-filament tape achieved the maximum value of 12420 A cm^{-2} when the dwell time in the first sintering is 40 h. As is well known, conditions for the first sintering, which decide the phase formation and microstructure have important influence on the J_c of the fully reacted tapes [20, 21]. The transversal cross-section images of the fully reacted mono-filament (Bi,Pb)-2223/Ag/Ni tapes with different dwell time in the first sintering are shown in Figs. 9(a–c). It is evidently observed that the tape dwelled for 30 h (Fig. 9(a)) in the first sintering process produces relatively few and small secondary phases grains while lots of large secondary phases particles appear in the samples with the annealing time of 40 h (Fig. 9(b)) and 50 h (Fig. 9(c)) in the first sintering. The presence of these large secondary phases may lead to a poor alignment of (Bi,Pb)-2223 grains. Combining Figs. 8 and 9, the lowest J_c of the tape that annealed for 40 h in the first sintering is attributed to the low (Bi,Pb)-2223 content and more secondary phases particles in this tape. Meanwhile, due to the large particles of secondary phases, the J_c of the tape with dwell time 50 h in the first sintering process is much lower than the tape annealed for 30 h in the first sintering even though it has the maximum fraction of the (Bi,Pb)-2223. What is more, except the tapes whose dwell time in the first sintering process is 30 h, the 61-filament tapes possess a higher J_c than that of the mono-filament tapes. This is absolutely due to the higher (Bi,Pb)-2223 fraction, better alignment of (Bi,Pb)-2223 grains and much more interfaces between the Ag layer and the ceramic cores in the 61-filament tapes. For 61-filament tapes, the diffusing of O_2 is much harder than that in the mono-filament tapes. Thus Bi-2223 content in some filaments, especially in the center of the tapes, is very low though that near the surface is higher than mono-filament tape (see Fig. 7a). The J_c of the 61-filament tape whose dwelling time in the first sintering is

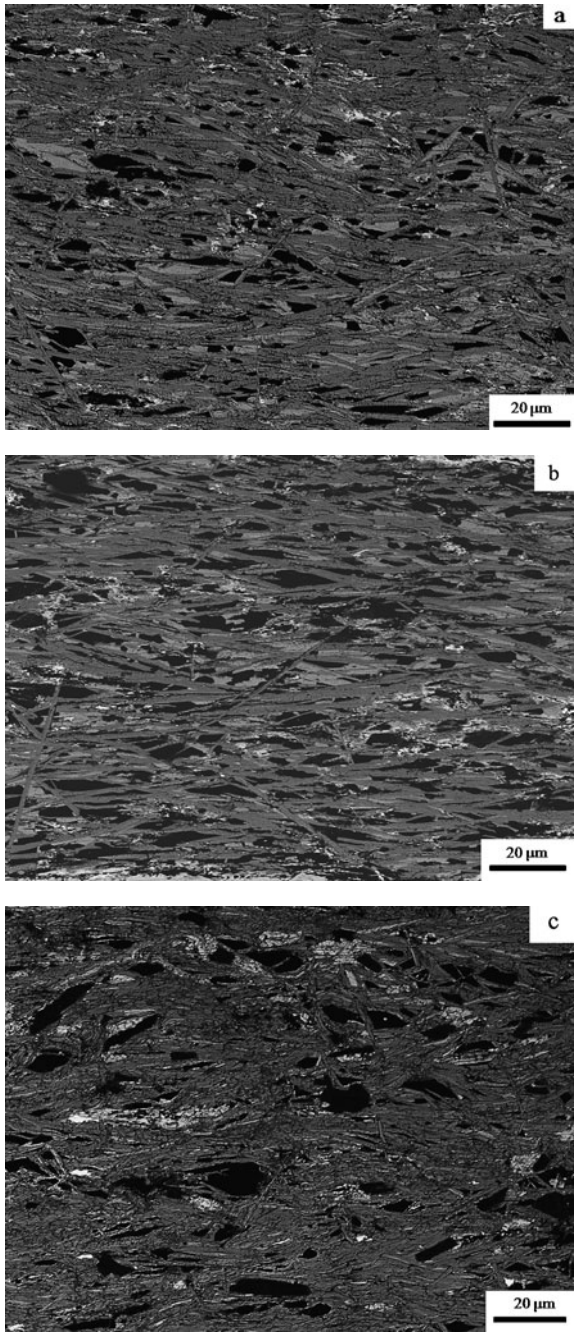

Fig. 9 The microstructures of fully reacted mono-filament Ag–Ni bimetallic sheathed (Bi,Pb)-2223 tapes with different dwell time in the first sintering: (**a**) 30 h, (**b**) 40 h, (**c**) 50 h

30 h is the lowest. A longer dwelling time is needed for 61-filament tapes to ensure a sufficient diffusing of O_2. Thus tape with dwelling time of 40 h in the first sintering has the highest J_c.

Studies on the mono- and multi-filament Ag–Ni bimetallic sheathed (Bi,Pb)-2223 tapes have made a breakthrough. But the shortcoming is that the J_c of them are much lower than the (Bi,Pb)-2223/Ag tapes. As a result, the sintering

conditions, especially the first sintering process, need to be further optimized. Though a preliminary study on the dwelling time in the first sintering has been finished, the sintering temperature, which is only determined by DSC method, will be further studied meticulously because the sintering temperature has the most crucial influence on the critical current density of the fully reacted tapes. Last but not the least, the producing technology of green tapes needs to be optimized as well because the phenomenon of inhomogeneous phase transformation was observed during the investigations. A significant improvement in the J_c of the Ag–Ni bimetallic sheathed (Bi,Pb)-2223 tapes may be achieved by optimizing the producing and sintering conditions.

4 Conclusion

Ag–Ni bimetallic sheathed mono-filament (Bi,Pb)-2223 tape with the J_c of 6656 A cm^{-2} and 61-filament tape with the J_c of 12420 A cm^{-2} have been fabricated by the PIT method. Fraction of the (Bi,Pb)-2223 increases with the sintering time extension, while alignment of the (Bi,Pb)-2223 grains has a better trend. Meanwhile, the 61-filament tapes have higher critical current densities due to a higher fraction and better alignment of (Bi,Pb)-2223 grains. The influences of the dwell time in the first sintering are preliminarily studied. The mono-filament tape whose dwell time in the first sintering is 30 h obtains the highest J_c while the 61-filament tape needs to dwell for 40 h in the first sintering process in order to reach the maximum.

Acknowledgements This work was supported by the National "863" program of China (No. 2009AA03Z202) and the Fundamental Research Funds for the Central Universities of China (Nos. CDJXS10131156 and CDJRC10130007).

References

1. Kato, T., Kobayashi, S., Yamazaki, K., Ohkura, K., Ueyama, M., Ayai, N.: Physica C **412–414**, 1066 (2004)
2. Osabe, G., Ayai, N., Kikuchi, M., Tatamidani, K., Nakashima, T., Fujikami, J., Kagiyama, T., Yamazaki, K., Yamade, S., Shizuya, E., Kobayashi, S., Hayashi, K., Sato, K., Shimoyama, J., Kitaguchi, H., Kumakura, H.: Physica C **470**, 1365 (2010)
3. Wojtasiewicz, G., Janowski, T., Kozak, S., Kondratowicz-kucewicz, B., Kozak, J., Surdachi, P., Glowacki, B.A.: Inst. Phys. Conf. Ser. **43**, 821 (2006)
4. Masuda, T., Yumura, H., Watanabe, M.: Physica C **468**, 2014 (2008)
5. Martini, L., Bocchi, M., Brambilla, R., Dalessandro, R., Ravetta, C.: IEEE Trans. Appl. Supercond. **19**, 1855 (2009)
6. Wu, S.T., Wu, Y., Song, Y.T., Wu, W.Y., Bi, Y.F., Xi, W.B., Xiao, L.Y., Wang, Q.L., Ma, Y.W., Liu, X.H.: IEEE Trans. Appl. Supercond. **19**, 1069 (2009)
7. Barik, S.K., Kwon, Y.K., Kim, H.M., Kim, S.H., Lee, J.D., Kim, Y.C., Park, H.J., Kwon, W.S., Park, G.S.: Cryogenics **49**, 271 (2009)
8. Al-Mosawi, M.K., Xu, B., Beduz, C., Yang, Y., Stephen, N.G.: Inst. Phys. Conf. Ser. **43**, 543 (2006)
9. Osamura, K., Sugrno, M.: Physica C **357–360**, 1128 (2001)
10. Osamura, K., Nyilas, A., Weiss, K.P., Shin, H.S., Katagiri, K., Ochiai, S., Hojo, M., Sugano, M., Ohsawa, K.: Cryogenics **51**, 21 (2011)
11. Scudiere, J.D., Buczek, D.M., Snitchler, G.L., Dipietro, P.J.: United States Patent: US5987342 (1999)
12. Salazar, A., Pastor, J.Y., Llorca, J.: IEEE Trans. Appl. Supercond. **14**, 1941 (2004)
13. Tsukamoto, O.: Supercond. Sci. Technol. **17**, S185 (2004)
14. Teranishi, R., Izumi, T., Shiohara, Y.: Supercond. Sci. Technol. **19**, S4 (2006)
15. Yamada, Y., Hattori, T.: Physica C **335**, 78 (2000)
16. Nemoto, Y., Fujii, H., Kitaguchi, H., Kumakura, H., Togano, K., Shima, K.: Physica C **350**, 69 (2001)
17. Grivel, J.C.: Supercond. Sci. Technol. **20**, 1059 (2007)
18. Ye, C.L., Li, M.Y., Chen, X.P., Sun, H.B., Zhu, X., Yu, L.: Physica C **471**, 1107 (2011)
19. Grasso, G., Jeremie, A., Flükiger, R.: Supercond. Sci. Technol. **8**, 827 (1995)
20. Parrell, J.A., Larbalestier, D.C., Dorris, S.E.: IEEE Trans. Appl. Supercond. **5**, 1275 (1995)
21. Chen, X.P., Yu, X.W., Xiao, R., Li, M.Y., Han, Z.: J. Alloys Compd. **209**, 1090 (2011)
22. Shinkawa, M., Utsunomiya, H., Sakai, T., Saito, Y.: Physica C **297**, 27 (1998)
23. Han, Z., Skov-Hansen, P., Freltoft, T.: Supercond. Sci. Technol. **10**, 371 (1997)
24. Luo, J.S., Merchant, N., Maroni, V.A., Riley, G.N., Czrter, W.L., Jr.: Appl. Phys. Lett. **63**, 690 (1993)
25. Mao, C.B., Zhou, L., Wu, X.Z., Sun, X.Y.: Physica C **281**, 159 (1997)
26. Chen, X.P., Li, M.Y., Liu, Q., Han, Z.: Physica C **469**, 116 (2009)
27. Horva, J., Guo, Y.C., Dou, S.X.: Physica C **271**, 59 (1996)
28. Grivel, J.C., Flükiger, R.: Supercond. Sci. Technol. **9**, 555 (1996)
29. Chen, X.P., Grivel, J.C., Li, M.Y., Liu, Q., Han, Z., Andersen, N.H., Homeyer, J.: Mater. Chem. Phys. **123**, 747 (2010)
30. Qu, T.M., Yang, X.P., Gu, C., Chen, X.P., Han, Z., Zeng, P.: Physica C **468**, 1767 (2008)